Hydrogen Molecules in the Small Dodecahedral Cage of a Clathrate Hydrate: Quantum Translation−Rotation Dynamics of the Confined Molecules

ARTICLE *in* THE JOURNAL OF PHYSICAL CHEMISTRY C · FEBRUARY 2007

Impact Factor: 4.77 · DOI: 10.1021/jp067318j

Hydrogen Molecules in the Small Dodecahedral Cage of a Clathrate Hydrate: Quantum Translation−Rotation Dynamics of the Confined Molecules

Francesco Sebastianelli, Minzhong Xu, Yael S. Elmatad, Jules W. Moskowitz, and Zlatko Bačić*

Department of Chemistry, New York University, New York, New York 10003

Received: November 6, 2006; In Final Form: December 14, 2006

We report the results of a rigorous theoretical study of the quantum translation−rotation (T−R) dynamics of one, two, and three H_2 and D_2 molecules confined inside the small dodecahedral $(H_2O)_{20}$ cage of the sII clathrate hydrate. For a single D_2 molecule, *o*- and *p*-D_2, in the small cage, accurate quantum five-dimensional (5D) calculations of the T−R energy levels and wave functions are performed by diagonalizing the 5D Hamiltonian which includes explicitly, as fully coupled, all three translational and the two rotational degrees of freedom of D_2, while the cage is taken to be rigid. These calculations provide a quantitative description of the quantum dynamics of D_2 inside the small cage and enable comparison with our quantum 5D results for the encapsulated H_2, *p*- and *o*-H_2, published very recently. The ground-state properties of one, two, and three *p*-H_2 and *o*-D_2 molecules in the small cage are calculated rigorously using the diffusion Monte Carlo method, with the emphasis on the quantum dynamics of two confined hydrogen molecules. The guest molecules are found to be effectively excluded from the sizable central region of the cage; they reside within a shell less than 2 bohrs wide and are additionally localized by the corrugation of the H_2−cage interaction potential. The two H_2 molecules are compressed, their mean distance inside the cage being much smaller than in the free H_2 dimer.

I. Introduction

Clathrate hydrates are a large group of inclusion compounds which trap guest molecules inside the polyhedral cavities of the host framework formed by hydrogen-bonded water molecules.[1] Several years ago, Mao et al.[2] reported the synthesis of clathrate hydrates with hydrogen molecules as guests. Because of the small size of H_2, very high pressures (typically 180−220 MPa at around 249 K) are required to stabilize these compounds. They have the classical structure II (sII), with 16 pentagonal dodecahedron (5^{12}) small cages and 8 hexakaidecahedron ($5^{12}6^4$) large cages per unit cell. The small and the large cages are formed by 20 and 28 H_2O molecules, respectively. Initially, it was estimated that two H_2 molecules occupy the small 5^{12} cage, while four H_2 molecules occupy the large $5^{12}6^4$ cage,[2] resulting in the reversible hydrogen-storage capacity of 5.3 wt %. This suggested that the hydrogen hydrate might be a promising hydrogen-storage material[3−5] and motivated numerous further studies of pure H_2[6] and binary clathrate hydrates.[7−11] A subsequent neutron diffraction study of the pure sII hydrogen hydrate[6] found only one D_2 molecule in the small cage and up to four D_2 molecules in the large cage. Single occupancy of D_2 in the small cage was also shown for the binary sII clathrate hydrate with tetrahydrofuran (THF) as the second guest, in high-resolution neutron diffraction experiments[10] and hydrogen-storage capacity studies.[11] The issue of single or double H_2 occupancy in the small cavities is important in determining the potential which the clathrate hydrates may have for the hydrogen storage.

There have been a number of theoretical investigations of the pure H_2[12−16] and the binary H_2−THF clathrate hydrate.[17] They have been largely concerned with the thermodynamic stability of the clathrates with a different number of H_2 molecules in the small and large cages. These studies have been inconclusive regarding the H_2 occupancy in the small cage, although most of them found double occupancy to be feasible. The treatment of the dynamics of the encapsulated hydrogen molecules has been limited to classical simulations. In one instance, the quantum zero-point vibrations of the cages and the host H_2 molecules were taken into account in the quasi-harmonic approximation in the calculations of the thermodynamic properties of hydrogen clathrate hydrate.[15]

One or more hydrogen molecules confined inside the small or large clathrate cage constitute a highly quantum mechanical system. Consequently, quantitative description of their quantum dynamics can be achieved only by solving exactly the multi-dimensional Schrödinger equation for the coupled translation−rotation (T−R) motions of the guest molecules. This has not been done in any of the theoretical studies mentioned above. The intriguing problem of the quantum dynamics of a hydrogen molecule in confined geometries has, to date, been investigated only for *p*- and *o*-H_2 on amorphous ice surfaces using quantum Monte Carlo simulations[18] and for H_2 within (rigid) carbon nanotubes by means of quantum four-dimensional (4D) calculations.[19−21]

This has prompted us to initiate a program of rigorous, systematic, and comprehensive theoretical investigations of the quantum dynamics of one or more hydrogen molecules inside the small and large cages of the clathrate hydrate. Besides addressing issues of experimental relevance, this will allow us to explore fundamental properties of highly quantum clusters confined in cavities of different shapes and sizes. In a very recent paper[22] (paper I), we reported the results of the first stage of

* Author to whom correspondence should be addressed. E-mail: zlatko.bacic@nyu.edu.

10.1021/jp067318j CCC: $37.00
Published on Web 01/24/2007

the program, the quantum five-dimensional (5D) bound-state calculations of the eigenstates of a single H_2 molecule, *p*- and *o*-H_2, inside the small dodecahedral (5^{12}) cage (subsequently referred to as "small''). The three translational and the two rotational degrees of freedom of the confined (rigid) H_2 were included explicitly as fully coupled, while the small cage was treated as rigid. The quantum mechanical T−R energy levels and wave functions of this 5D system were calculated exactly for the realistic, highly anharmonic, and anisotropic H_2−cage potential energy surface (PES) employed, by diagonalizing the 5D T−R Hamiltonian. From this emerged the first quantitative picture of the quantum T−R dynamics of H_2 in the small cage, revealing that j is a good rotational quantum number, negative anharmonicity of excited translational modes, lifting of the threefold degeneracy of the $j = 1$ rotational level, and considerable translational−rotational coupling.[22]

In this paper, our investigations are extended in two directions. First, accurate quantum 5D calculations of T−R energy levels and wave functions are performed for a single D_2 molecule, *o*- and *p*-D_2, inside the small dodecahedral cage, using the methodology described in paper I. D_2 and H_2 differ greatly by mass and rotational constants, which results in quantitatively different T−R dynamics of the two encapsulated molecules. Second, the ground-state properties, energetics, and vibrationally averaged structural information are calculated rigorously for one, two, and three *p*-H_2 and *o*-D_2 molecules in the small cage, using the diffusion Monte Carlo (DMC) method. The focus here is on the quantum T−R dynamics of two confined hydrogen molecules and how it differs from the quantum behavior of a single H_2 in the dodecahedral cavity. The DMC calculations do illuminate a number of interesting and important facets of the quantum dynamics of a pair of hydrogen molecules inside the small cage.

Section II describes the cage geometry, PESs, and the computational methodology employed in the present study. The results are presented and discussed in section III, and the conclusions are given in section IV.

II. Theory

In this study, as in paper I,[22] the small cage is assumed to be rigid, while the quantum dynamics of the confined hydrogen molecules is treated rigorously. We believe that this model is appropriate and retains the key features of the dynamical problem at hand for reasons given previously:[22] (a) the guest H_2 molecule is much lighter than the $(H_2O)_{20}$ host cage, (b) the interaction of the hydrogen molecule with the cage is much weaker than the hydrogen bonds between the H_2O molecules of the cage, (c) the water molecules of the cage are each hydrogen bonded to three neighboring molecules, creating a fairly rigid framework, and (d) in the clathrate hydrate, the cage is embedded in an extended lattice, which can only enhance its rigidity.

A. Cage Geometry and PESs. The small dodecahedral $(H_2O)_{20}$ cage has been defined in paper I, and its geometry can be seen in Figure 1. The water molecules forming the cage have the geometry employed in the calculations of 5D (rigid-monomer) PES for the H_2O−H_2 complex[23] used by us to construct the H_2-cage PES described below; the O−H bond length is 1.836 au and the H−O−H angle is 104.69°. The oxygen atoms were arranged according to Patchkovskii and Tse:[12] 8 oxygen atoms occupy the corners of a perfect cube (O_h), at the distance of 7.24 au from the cage center, while the remaining 12 oxygen atoms, 7.48 au from the center of the cage, are arranged so as to transform according to the T_h subgroup of

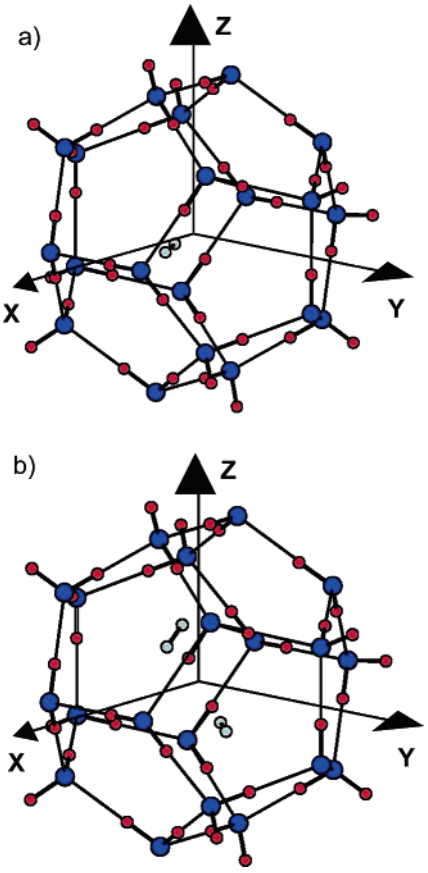

Figure 1. Small dodecahedral cage with (a) one and (b) two hydrogen molecules in their equilibrium configurations. The Cartesian *X*, *Y*, and *Z* coordinate axes shown coincide with the three principal axes of the cage.

O_h. This configuration of the O atoms corresponds closely to that from the X-ray diffraction experiments for the sII clathrate hydrates.[24] However, the H atoms of the water molecules are configurationally disordered. There is one H atom on each edge of the cage, forming a hydrogen bond between two O atoms at the corners connected by the edge. Since the dodecahedron has 30 edges, 10 water molecules are double donors, with both their H atoms participating in the hydrogen bonds with two neighboring O atoms. The other 10 water molecules are single donors, having only one H atom in a hydrogen bond, while the second O−H bond of the molecule is free, dangling from the surface of the cage. There are over 30 000 possible hydrogen-bonding topologies for a dodecahedral $(H_2O)_{20}$ cage.[25] The one used in paper I and here, shown in Figure 1, was constructed by aiming to distribute the nonbonded O−H bonds rather evenly over the cage exterior and to maximize the hydrogen-bonding network.

In this work, small $(H_2/D_2)_n$ clusters, $n = 1-3$, inside the cage are considered. All interactions, among the hydrogen molecules of the cluster (for $n > 1$) as well as those between the hydrogen molecule(s) and the rigid cage, are assumed to be pairwise additive. Hence, the total PES for a $(H_2)_n$ cluster in the dodecahedral cavity has the form

$$V(\mathbf{Q}) = \sum_{i=1}^{n} V_{H_2-\text{cage}}(\mathbf{q}_i) + \sum_{i<j}^{n} V_{H_2-H_2}(\Omega_{ij}) \qquad (1)$$

where $\mathbf{Q}$ is the vector defining the coordinates of all the cluster particles, $\mathbf{q}_i$ are the (Cartesian) coordinates of the *i*th H_2 molecule within the cage, and Ω_{ij} are the intermolecular diatom−diatom Jacobi coordinates describing the mutual orientation of the pair

of H_2 molecules *i* and *j*. In eq 1, the first term accounts for the (additive) interaction of each H_2 molecule with the cage, and the second term represents the interactions (also additive) between all pairs of H_2 molecules. The 5D PES for a (rigid) H_2 molecule within the small cage was described already in paper I. It is pairwise additive, generated by summing over the interactions between the H_2 molecule and each of the 20 water molecules forming the cage. For the pair interaction between H_2 and H_2O, we use the high-quality ab initio 5D (rigid monomer) PES for the H_2-H_2O complex by Hodges and co-workers,[23] whose global minimum is at -240.8 cm^{-1}. This requires the transformation of the H_2 Cartesian coordinates $\mathbf{q}_i$ to the Jacobi-like internal coordinates used for this H_2-H_2O PES. In fact, for any given $\mathbf{q}_i$, the transformation has to be done 20 times, once for each H_2O molecule of the cage. The H_2-H_2 pair potential is described by the ab initio 4D (rigid monomer) PES by Diep and Johnson,[26] used by us previously in the theoretical studies of HF-doped clusters of molecular hydrogen.[27,28] Its global minimum lies at -40.00 cm^{-1}.

B. Bound-State Calculations. *1. Quantum 5D Calculations of T−R Eigenstates*. For a single hydrogen molecule inside the (rigid) cage, ground and excited T−R energy levels and wave functions are calculated as fully coupled and numerically exact for the PES employed using the methodology presented in paper I, which is summarized here. The set of five coordinates (x, y, z, θ, ϕ) is employed; x, y, and z are the Cartesian coordinates of the center of mass (c.m.) of the hydrogen molecule, while the two polar angles θ and ϕ specify its orientation. The origin of the coordinate system is at the c.m. of the cage, and its axes, shown in Figure 1a, are aligned with the principal axes of the cage. Relative to a hydrogen molecule, the cage can be assumed to be infinitely heavy and non-rotating. Then, the 5D Hamiltonian for the T−R motions of the guest (hydrogen) molecule is

$$H = -\frac{\hbar^2}{2m}\left(\frac{\partial^2}{\partial x^2}+\frac{\partial^2}{\partial y^2}+\frac{\partial^2}{\partial z^2}\right) + B\mathbf{j}^2 + V(x, y, z, \theta, \phi) \tag{2}$$

In eq 2, m is the mass of the hydrogen molecule, while B and $\mathbf{j}^2$ are the rotational constant and the angular momentum operator of the diatomic, respectively. $V(x, y, z, \theta, \phi)$ in eq 2 is the 5D PES described in the preceding section. The energy levels and wave functions of the 5D Hamiltonian in eq 2 are obtained without any dynamical approximations, using the computational methodology developed by us for the 5D intermolecular vibrational eigenstates of Ar_nHF clusters,[29−32] where the Ar_n subunit was treated as rigid. A detailed description of the method can be found in ref 30. In brief, this methodology relies on the three-dimensional (3D) direct-product discrete variable representation (DVR)[33,34] for the x, y, and z coordinates and the spherical harmonics for the angular, θ, and ϕ coordinates. The sequential diagonalization and truncation procedure of Bačić and Light[33,35,36] is utilized to reduce drastically the size of the final Hamiltonian matrix, without loss of accuracy. Diagonalization of this truncated Hamiltonian matrix yields the desired 5D T−R energy levels and wave functions.

In the quantum 5D calculations of the T−R eigenstates of *o*- and *p*-D_2 inside the small cage reported in this paper, the rotational constant for D_2 in eq 2 has the value $B = 29.9037$ cm^{-1}.[37,38] The dimension of the sine-DVR basis was 50 for each of the three Cartesian coordinates x, y, and z. The sine-DVR grid spanned the range -2.65 au $\le \lambda \le 2.65$ au ($\lambda = x, y, z$). The angular basis included functions up to $j_{max} = 5$. The energy cutoff parameter for the intermediate 3D eigenvector basis[30] was set to 880 cm^{-1}, resulting in the final full 5D Hamiltonian matrix of dimension 7700.

2. DMC Calculations of Ground-State Properties. When two or more hydrogen molecules are confined inside the cage, the dimensionality of the bound-state problem currently precludes the calculation of their excited T−R eigenstates. We hope to overcome this obstacle, but our effort in this direction is in an early stage. Therefore, the ground-state properties of (p-H_2/o-D_2)$_n$ clusters with $n = 1-3$ inside the small cage were calculated rigorously for the PESs employed using the DMC method originally developed by Anderson.[39,40] This approach exploits the analogy between the time-dependent Schrödinger equation for the imaginary time $\tau = it$ and the diffusion equation with an additional source/sink term, which allows the former to be solved by a random walk. Detailed descriptions of the DMC method are available in the literature.[41−44] Our implementation of the DMC methodology has been discussed previously.[27,28] The hydrogen molecules are treated as rigid, their bond lengths held fixed by means of the constraint dynamics method of Sarsa and co-workers.[45] The rotational constants used are $B_{H_2} = 59.322$ cm^{-1} and $B_{D_2} = 29.904$ cm^{-1};[37,38] these same values were of course employed in the quantum 5D calculations. The vibrationally averaged spatial distribution of H_2 (i.e., p-H_2 and o-D_2) molecule(s) within the cage is characterized by means of the probability distribution functions (PDFs) of the following two coordinates: $\vec{R}_i$, the vector connecting the c.m. of the cage with the c.m. of the ith H_2 molecule, and $\vec{r}_{ij}$, the vector connecting the centers of mass of H_2 molecules i and j (for $n > 1$). The corresponding one-dimensional (1D) PDFs and their normalizations are

$$P(R) = \frac{1}{n}\sum_{i=1}^{n}\langle\delta(|\vec{R}_i| - R)\rangle \qquad \int_0^\infty P(R)\,\mathrm{d}R = 1 \tag{3}$$

$$P(r) = \frac{1}{(1/2)n(n-1)}\sum_{i<j}^{n}\langle\delta(|\vec{r}_{ij}| - r)\rangle \qquad \int_0^\infty P(r)\,\mathrm{d}r = 1 \tag{4}$$

In addition, a 3D PDF of the Cartesian cordinates of the centers of mass of H_2 molecules, $P(x, y, z)$, is defined:

$$P(x, y, z) = \frac{1}{n}\sum_{i=1}^{n}\langle\delta(x_i - x)\,\delta(y_i - y)\,\delta(z_i - z)\rangle$$
$$\int_{-\infty}^{\infty}\int_{-\infty}^{\infty}\int_{-\infty}^{\infty}\mathrm{d}x\,\mathrm{d}y\,\mathrm{d}z\,P(x, y, z) = 1 \tag{5}$$

The DMC calculations reported here use an ensemble of 1500 walkers and the time step of 1.0 au. For $n = 1$ and 2, the simulations involve 10 independent runs, while for $n = 3$ only one run is performed. In every run, after the initial equilibration, the ensemble is propagated in 120 blocks consisting of 2000 steps each.

III. Results and Discussion

A. Quantum T−R Dynamics of D_2 Molecule in the Small Cage. Like hydrogen, molecular deuterium exists in two species, *o*- and *p*-D_2, for which the rotational quantum number j has only even ($j = 0, 2, 4, ...$) and odd ($j = 1, 3, 5, ...$) values, respectively. The lower-lying quantum 5D T−R energy levels of *o*-D_2 and *p*-D_2 in the dodecahedral cage are given in Tables 1 and 2, respectively, together with their Cartesian (translational) quantum number assignments (υ_x, υ_y, υ_z) and, for *p*-D_2 in Table 2, the rotational quantum numbers (j, $|m|$). Table 1 also displays for each state the root-mean-square (rms) amplitudes Δx, Δy,

TABLE 1: Lowest Nine Excited T−R Energy Levels of an *o*-D_2 Molecule in the Small Dodecahedral Cavity of the Clathrate Hydrate, from the Quantum 5D Bound-State Calculations[a]

n	E	ΔE	Δx	Δy	Δz	$(\upsilon_x, \upsilon_y, \upsilon_z)$
0	−740.754	0.00	0.71	0.60	0.55	(0, 0, 0)
1		28.67	1.08	0.58	0.52	(1, 0, 0)
2		39.51	0.67	0.95	0.54	(0, 1, 0)
3		49.06	0.65	0.58	0.89	(0, 0, 1)
4		70.73	1.17	0.68	0.52	(2, 0, 0)
5		75.59	1.04	0.83	0.54	(1, 1, 0)
6		84.43	1.01	0.58	0.84	(1, 0, 1)
7		89.79	0.64	1.10	0.61	(0, 2, 0)
8		96.41	0.64	0.87	0.87	(0, 1, 1)
9		109.07	0.65	0.63	1.01	(0, 0, 2)

[a] They all correspond to the $j = 0$ state of *o*-D_2. The excitation energies ΔE are relative to the lowest even-j level designated $n = 0$, whose energy E is listed. All energies are in cm^{-1}. Also shown are the rms amplitudes Δx, Δy, and Δz (in a.u.) and the Cartesian quantum number assignments $(\upsilon_x, \upsilon_y, \upsilon_z)$.

TABLE 2: Lowest Ten Excited T−R Energy Levels of a *p*-D_2 Molecule in the Small Dodecahedral Cavity of the Clathrate Hydrate from the Quantum 5D Bound-State Calculations[a]

n	E	ΔE		$(\upsilon_x, \upsilon_y, \upsilon_z)$	$(j, \lvert m\rvert)$
0	−706.161	**0.00**		**(0, 0, 0)**	**(1, 0)**
1		**25.62**	[0.00]	**(0, 0, 0)**	**$(1, 1)_l$**
2		30.66		(1, 0, 0)	(1, 0)
3		38.82		(0, 1, 0)	(1, 0)
4		52.02		(0, 0, 1)	(1, 0)
5		55.19	[29.57]	(1, 0, 0)	$(1, 1)_l$
6		**60.00**		**(0, 0, 0)**	**(1, 1)u**
7		68.93	[43.30]	(0, 1, 0)	$(1, 1)_l$
8		72.58		(2, 0, 0)	(1, 0)
9		74.94		(1, 1, 0)	(1, 0)
10		77.26	[51.63]	(0, 0, 1)	$(1, 1)_l$

[a] The excitation energies ΔE are relative to the lowest odd-j level designated $n = 0$, whose energy E is listed. Also shown are the Cartesian $(\upsilon_x, \upsilon_y, \upsilon_z)$ and the rotational $(j, |m|)$ quantum number assignments. The energies in [ ] brackets are relative to the $(\mathbf{1},\mathbf{1})_\mathbf{l}$ state (0, 0, 0) [$n = 1$]. They are the translational fundamentals for $(\mathbf{1},\mathbf{1})_\mathbf{l}$. All energies are in cm^{-1}.

and Δz; the rms amplitudes are not shown in Table 2, since they are very similar for the T−R states of *o*-D_2 and *p*-D_2 with the same Cartesian quantum numbers $(\upsilon_x, \upsilon_y, \upsilon_z)$. The quantum number assignments were made in the same way as for *p*-H_2 and *o*-H_2 in paper I.[22] The Cartesian quantum numbers were in most cases assigned on the basis of the rms amplitudes and confirmed by inspecting the plots of the 3D reduced probability density in (x, y, z). The rotational quantum numbers $(j, |m|)$ were assigned by projecting an eigenstate on the rotational basis and with the help of the 2D reduced probability density in the angular coordinates (θ, ϕ).[22]

The T−R dynamics of D_2 in the small cage manifests all of the key features that we observed for the encapsulated H_2 molecule, described in paper I. To begin with, j is a good quantum number for all of the T−R eigenstates of D_2 considered. The states of *o*-D_2 in Table 1 are 93−95% $j = 0$ states. In the case of *p*-H_2, the $j = 0$ state contribution was a bit higher, 98−99%.[22] The *p*-D_2 states shown in Table 2 are 99% $j = 1$ states; the same was found for the T−R states of *o*-H_2 in the small cage.[22]

From Table 1, the frequencies of the x mode fundamental (1, 0, 0), the y mode fundamental (0, 1, 0), and the z mode fundamental (0, 0, 1) of *o*-D_2 are 28.7, 39.5, and 49.1 cm^{-1}, respectively. They are a factor of 0.5−0.6 smaller than the corresponding fundamentals of *p*-H_2, which are 52.4, 66.8, and 77.7 cm^{-1}, respectively.[22] For both *o*-D_2 and *p*-H_2, the frequency spread of their fundamentals arises from the nonsymmetric arrangement of the H atoms in the hydrogen-bonding network of the cage. The ordering of the excited translational energy levels of *o*-D_2 is the same as that for *p*-H_2 (Table 1 of paper I), but their energies are very different because of the large difference in the masses of the two isotopomers. The translational modes of *o*-D_2 (and *p*-D_2 in Table 2) display negative anharmonicity, observed also for those of *p*-H_2 and *o*-H_2;[22] the frequencies of the first-overtone states (2, 0, 0), (0, 2, 0), and (0, 0, 2) are more than twice the frequencies of the respective fundamentals.

TABLE 3: Ground-State Energies of $(p\text{-}H_2)_n$ and $(o\text{-}D_2)_n$ Clusters ($n = 1-3$) inside the Small Dodecahedral Cage, Denoted $E_{0,n}$, from the DMC Calculations[a]

n	$E_{0,n}$	$V_{\min,n}$	ZPE_n	$\mathrm{ZPE}_n/\lvert V_{\min,n}\rvert$
1	-707.61 ± 0.08 (-740.63 ± 0.07)	−884.8	177.2 (144.2)	0.20 (0.16)
2	-194.45 ± 0.35 (-425.11 ± 0.29)	−1095.2	900.8 (670.1)	0.82 (0.61)
3	1494.98 ± 2.26 (1125.37 ± 2.06)	−239.4	1734.4 (1364.8)	

[a] Also shown are the global minima of the encapsulated $(H_2)_n$ clusters, $V_{\min,n}$, the ZPEsof their coupled translational and rotational motions, ZPE_n, and the ratios $\mathrm{ZPE}_n/|V_{\min,n}|$. For all the quantities shown, the numbers in parentheses are for the $(o\text{-}D_2)_n$ clusters. All energies are in cm^{-1}.

The anisotropy of the cage environment lifts completely the threefold degeneracy of the $j = 1$ rotational level of *p*-D_2, as evident from Table 2. For the ground translational state (0, 0, 0), the states $(1, 1)_l$ ($n = 1$) and $(1, 1)_u$ ($n = 6$) lie 25.62 and 60.00 cm^{-1}, respectively, above the (1, 0) state ($n = 0$). These splittings are remarkably similar to the ones found for *o*-H_2, 26.91 and 60.57 cm^{-1}, respectively.[22] In paper I, we showed for *o*-H_2 that the calculated $j = 1$ level splittings could be reproduced accurately by the simple model which considers only the angular (θ, ϕ) degrees of freedom of the problem. The guest molecule is placed at the center of the cage and the angular part of the H_2−cage PES is averaged over the rotational wave functions of (1, 0), $(1, 1)_l$, and $(1, 1)_u$ states. Since the rotational wave functions are the same for *p*-D_2 and *o*-H_2, the model predicts that the splitting of the $j = 1$ states should be very similar for the two molecules, which is borne out of our results.

While for (0, 0, 0) the T−R coupling is weak, it does increase for excited translational states of D_2. This manifests in the variation of the x, y, and z mode fundamentals with the rotational quantum numbers $(j, |m|)$. Thus, for (0,0) (Table 1), the x, y, and z mode fundamentals are 28.7, 39.5, and 49.1 cm^{-1}, respectively, while for (1,0) (Table 2), they are 30.7, 38.8, and 52.0 cm^{-1}, respectively.

B. Ground-State Properties of 1−3 Hydrogen Molecules Inside the Small Cage. The results discussed in the preceding section, together with our findings reported in paper I, provide a comprehensive description of the quantum T−R dynamics of one H_2 or D_2 molecule inside the small cage. This section presents the results of the DMC calculations for one, two, and three *p*-H_2 and *o*-D_2 molecules. The main focus of the discussion is on the ground-state quantum dynamics of two hydrogen molecules confined to the small cage.

The DMC ground-state energies $E_{0,n}$ of $(p\text{-}H_2)_n$ and $(o\text{-}D_2)_n$ ($n = 1-3$) clusters in the small dodecahedral cage are shown in Table 3, together with global minima $V_{\min,n}$ of the encapsulated $(H_2)_n$ clusters and the zero-point energies (ZPEs) of the coupled translational and rotational motions of the hydrogen

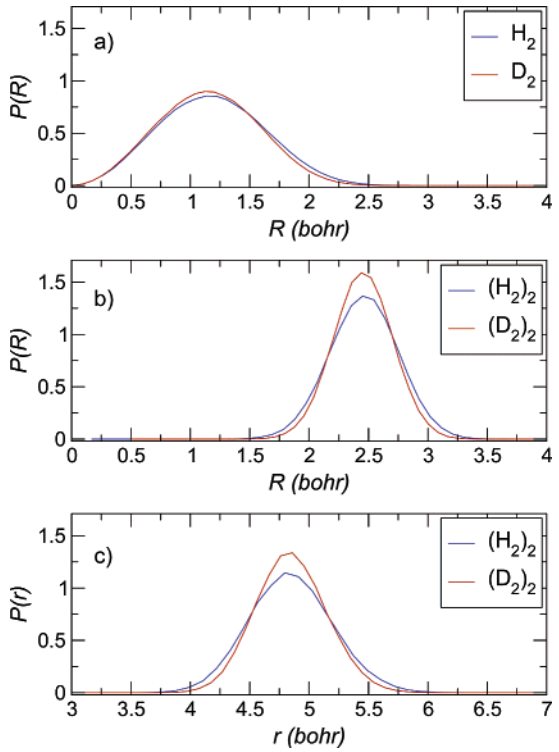

Figure 2. Cage center to p-H_2/o-D_2 c.m. distance (R) probability distribution $P(R)$ for (a) one p-H_2/o-D_2 molecule and (b) two p-H_2/o-D_2 molecules. The p-H_2−p-H_2 and o-D_2−o-D_2 c.m. distance (r) probability distributions $P(r)$ for two p-H_2 and two o-D_2 molecules in the small cage, respectively, are shown in (c).

molecule(s). The ZPEs are obtained as $\mathrm{ZPE}_n = E_{0,n} - V_{\mathrm{min},n}$. For $n = 1$ and 2, the ground-state energies are negative. These states are truly bound since they are lower in energy than the hydrogen molecule(s) at infinite separation from the cage, which is taken as the zero of the energy. In contrast, for $n = 3$, the ground-state energies are large and positive for both isotopomers. Thus, these states are metastable, confined within the cage by high barriers in all directions. The probability that in the course of the random-walk simulation a walker will escape the cage is very small; consequently, the DMC simulations converge to the ground state without any special effort. In the following, we mainly discuss the results obtained for $n \leq 2$. The ground-state energy of a single p-H_2 molecule inside the cage from the DMC calculations, -707.61 ± 0.08 cm^{-1}, is in excellent agreement with the value of -707.60 cm^{-1} from our quantum 5D bound-state calculations of the coupled T−R eigenstates.[22] The same is true for the o-D_2 molecule in the small cage; the DMC ground-state energy, -740.63 ± 0.07, agrees very well with the quantum 5D result in Table 1, -740.75 cm^{-1}.

It is evident from Table 3 that the ground-state energy increases rapidly with the number of encapsulated p-H_2 or o-D_2 molecules. In going from $n = 1$ to $n = 2$, the ground-state energy grows from -707.6 to -194.5 cm^{-1} for p-H_2 and grows from -740.6 to -425.1 cm^{-1} in the case of o-D_2. This is due primarily to the extremely sharp rise of the ZPE which accompanies the introduction of the second hydrogen molecule into the cage. As Table 3 shows, for p-H_2 there is a *fivefold* increase of the ZPE, from 177.2 cm^{-1} for $n = 1$ to 900.8 cm^{-1} for $n = 2$; in the case of o-D_2, the ZPE increases by a factor of 4.7, from 144.2 cm^{-1} for $n = 1$ to 670.1 cm^{-1} for $n = 2$. The ZPE per p-H_2 (o-D_2) molecule, 450.4 cm^{-1} (335.1 cm^{-1}), for $n = 2$ is 2.5 (2.3) times greater than the ZPE of a single p-H_2 (o-D_2) molecule in the cage. When the third hydrogen molecule is added, to p-H_2 or o-D_2, the ZPE roughly doubles relative to

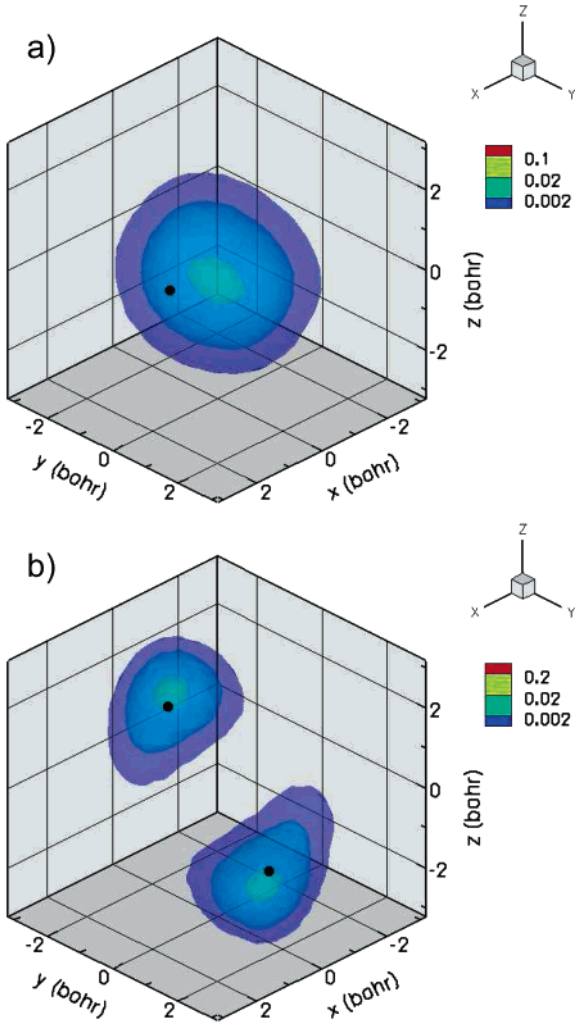

Figure 3. 3D p-H_2 c.m. probability distribution $P(x, y, z)$ for (a) one and (b) two p-H_2 molecules in the small cage. The black dot(s) correspond to the minimum-energy configuration of one and two hydrogen molecules (their centers of mass), respectively, which are shown in Figure 1.

the $n = 2$ values. With one p-H_2 inside, the ZPE is 20% of the well depth (16% for o-D_2), while for two p-H_2 molecules, the ZPE represents 82% of the well depth (61% for o-D_2). For $n = 3$, the ZPE is much greater than the potential well depth, and the ground state is quasi-bound.

The explanation for the large jump in the ZPE (total and per H_2 molecule) from $n = 1$ to $n = 2$ can be found in the PDFs displayed in Figures 2 and 3, which reveal the spatial distribution of one and two hydrogen molecules confined inside the small cage. For $n = 1$, the cage center to p-H_2/o-D_2 c.m. distance (R) probability distribution $P(R)$ in Figure 2a goes to zero at the center of the cage ($R = 0$) because of the vanishing volume element and peaks at $R \sim 1.2$ bohr. Its substantial width reflects the large-amplitude translational motions of the p-H_2/o-D_2 molecule inside the cage. $P(R)$ for $n = 2$ (Figure 2b) looks qualitatively different. Its peak has shifted to $R \sim 2.5$ bohr, and $P(R)$ is essentially zero for $R < 1.5$ bohr and also for $R > 3.5$ bohr. Hence, the two hydrogen molecules are virtually excluded from the central region of the cage with the diameter of ~3 bohr and reside within a shell less than 2 bohr wide.

A complementary view is provided by the p-H_2−p-H_2 and o-D_2−o-D_2 c.m. distance (r) probability distributions $P(r)$ for $n = 2$ shown in Figure 2c, which have a peak around 4.9 bohr; the expectation value of r is ~4.85 bohr. Thus, the picture

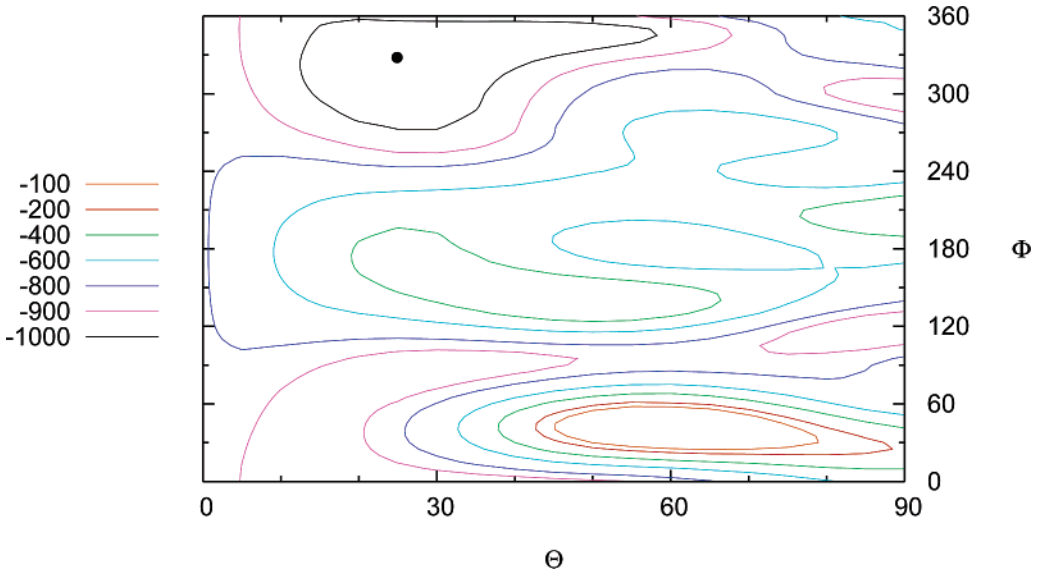

Figure 4. Contour plot of $V_{min}(\Theta, \Phi)$, the potential energy of two H_2 molecules inside the cage (in cm^{-1}). Θ and Φ are the polar and azimuthal angles, respectively, of the vector that connects the centers of mass of the two H_2 molecules and passes through the center of the cage. Its length is fixed at 4.84 bohr, the equilibrium distance between the centers of mass of the guest molecules in the global minimum for $n = 2$. At every point (Θ, Φ), the total potential is minimized with respect to all other coordinates defining the orientation of the two H_2 molecules relative to one another and to the water molecules of the cage. For further details, see the text.

which, for $n = 2$, emerges from considering the PDFs $P(R)$ and $P(r)$ is that of two *p*-H_2 or two *o*-D_2 molecules at the average distance of 4.85 bohr from one another, restricted to a rather narrow range of distances from the center of the cage, $1.5 < R < 3.5$ bohr ($\langle R \rangle = 2.45$ bohr). The two hydrogen molecules confined inside the small cage are substantially compressed. Their mean distance of ~4.85 bohr in the cage is much smaller than in the free H_2 dimer; on the ab initio 4D (rigid monomer) H_2-H_2 PES[26] that we use, the equilibrium separation between the two monomers is 6.33 bohr, while its expectation value is 10.67 bohr (from our DMC calculations of the free *p*-H_2 dimer). Therefore, the interaction between the two H_2 molecules in the small cage is repulsive. At $r = 4.85$ bohr, the value of the H_2-H_2 PES (minimized with respect to the three angular coordinates of the dimer) is 219.5 cm^{-1}, compared to -40.0 cm^{-1} at its global minimum. But, the H_2-H_2 repulsion is compensated by the strong attractive interaction of the H_2 molecules with the cage. Consequently, the global minimum of two encapsulated H_2 molecules shown in Table 3, -1095 cm^{-1}, is lower in energy than that of $n = 1$, -884.8 cm^{-1}. However, the sharp increase in the ZPE from $n = 1$ to $n = 2$, discussed above, exceeds by far the lowering of the potential energy so that the $n = 2$ ground-state energy is much higher than the ground-state energy for $n = 1$.

The two hydrogen molecules inside the small cage are in fact localized to a greater degree than indicated by $P(R)$ and $P(r)$ for $n = 2$ in Figure 2. This is revealed by the 3D PDF $P(x, y, z)$ of the center(s) of mass of the *p*-H_2 molecule(s) displayed for $n = 1$ and 2 in Figure 3. For $n = 1$, $P(x, y, z)$ is essentially spherical, spread uniformly around the center of the cage. In contrast, $P(x, y, z)$ for $n = 2$ features two distinct lobes. Each lobe is centered at the position of the c.m. of one hydrogen molecule in the global minimum for $n = 2$ shown in Figure 1b and corresponds to the large-amplitude motions of a *p*-H_2 molecule rather localized in the neighborhood of its respective equilibrium coordinates. It is this localization of the two hydrogen molecules to a relatively small portion of the interior of the cage that is responsible for the conspicuously large increase in the ZPE upon the encapsulation of the second H_2 molecule. A single guest H_2 has a much greater volume of space accessible to it, resulting in its relatively small ZPE.

The localization of the two H_2 molecules evident from Figure 3b is somewhat surprising. In view of the apparent high symmetry of the cage and $P(R)$ in Figure 2, one might expect a fairly uniform angular distribution of the two guest molecules within a spherical shell, for $1.5 < R < 3.5$ bohr. However, it turns out that when the hydrogen molecules are forced closer to the walls of the cage by their mutual repulsion, the interior surface of the cage that they interact with is not smooth; instead, they see it as rough, corrugated, with significant angular variations. This is made visible by Figure 4, which shows a 2D contour plot of the potential energy of two H_2 molecules inside the cage as a function of two angles Θ and Φ, generated as follows. Θ and Φ are the spherical polar and azimuthal angles, respectively, of the vector that connects the centers of mass of the two H_2 molecules and passes through the center of the cage. Its length is fixed at 4.84 bohr, the equilibrium distance between the centers of mass of the guest molecules in the global minimum for $n = 2$. Over the range of Θ and Φ, this vector sweeps a sphere with the radius of $4.84/2 = 2.42$ bohr. It is sufficient to vary Θ from 0 to 90°; since the vector connects both H_2 molecules, specifying its coordinates in the upper half of the sphere defines uniquely those of the other end, in the lower hemisphere ($90° < \Theta < 180°$). At each point (Θ, Φ), the total potential is minimized with respect to all other coordinates defining the orientation of the two H_2 molecules relative to one another and to the water molecules of the cage. The resulting potential denoted $V_{min}(\Theta, \Phi)$ is displayed in Figure 4. Clearly, $V_{min}(\Theta, \Phi)$ is not smooth; on the contrary, it is rugged, that is, varies strongly with Θ and Φ. This rugged potential landscape experienced by the two guest H_2 molecules arises from the configurational disorder of the H atoms of the water molecules forming the cage. The $n = 2$ global minimum, marked by a black dot in Figure 4, lies in a low-energy basin of $V_{min}(\Theta, \Phi)$, which is sufficiently deep to localize the ground-state wave function, giving rise to the two lobes seen in Figure 3b.

Finally, what do our DMC results say about the H_2 occupancy in the small dodecahedral cage? They clearly rule out having

three hydrogen molecules in the small cage. On the other hand, they indicate the possibility of double occupancy in the small cage. On this point, our DMC calculations agree with the majority of the theoretical treatments published to date,[12,13,15−17] none of which treated the quantum dynamics of the guest molecules. From the DMC calculations, two *p*-H_2 and *o*-D_2 molecules are bound inside the cage by 194 and 425 cm^{-1}, respectively. A caveat could be made that the DMC results are for $T = 0$ K, while the experimental data are obtained at higher temperatures. But, the most recent neutron-diffraction experiments on the pure[6] and binary[10] hydrogen clathrates were performed at very low temperatures as well. In particular, the neutron-diffraction study of the binary THF−H_2 clathrate hydrate,[10] which reported only single D_2 occupancy of the small dodecahedral cavities, was carried out at 20 K. We do not believe that the quantum dynamics of two guest hydrogen molecules changes so profoundly from 0 to 20 K as to make the $T = 0$ K DMC predictions inapplicable to the experimental conditions. In this context, it can be mentioned that at 20 K a single hydrogen molecule in the cage is almost exclusively in the ground T−R state. Some uncertainty regarding the DMC predictions about the H_2 occupancy stems also from our treatment of the cage as rigid and the pairwise-additive H_2−cage PES employed. The impact of these two factors is hard to quantify. The vibrations of the host framework of water molecules should not play a major role at very low temperatures. The H_2−cage interaction potential is based on the best available ab initio 5D H_2−H_2O PES.[23] The pairwise-additivity assumption undoubtedly introduces some error, but we do not expect it to be large enough to change the occupancy results qualitatively, especially for two D_2 molecules in the cage. The definitive assessment of the accuracy of the present model with respect to its prediction of the maximum H_2 occupancy in the small cage must await future theoretical work which should include the cage vibrations and/or improved H_2−cage interactions, while retaining the rigorous description of the T−R dynamics of the guest molecules achieved in this study and extending it to the $T > 0$ K situation.

IV. Conclusions

We have performed a rigorous investigation of the quantum T−R dynamics of one, two, and three H_2 and D_2 molecules inside the small dodecahedral cage of the sII clathrate hydrate. The cage was taken to be rigid. For a single D_2 molecule (*o*-D_2 and *p*-D_2) in the small cage, excited T−R energy levels and wave functions were calculated accurately in five dimensions, as fully coupled. The main features which emerged, such as j being a good quantum number, negative anharmonicity of the translational modes, and lifting of the threefold degeneracy of the $j = 1$ rotational level, were identified by us previously for *p*-H_2 and *o*-H_2 in the small cage.[22] But the T−R eigenstates of D_2 and H_2 have very different energies because of the large difference between the masses and the rotational constants of the two isotopomers.

In addition, the ground-state properties for $n = 1-3$ *p*-H_2 and *o*-D_2 molecules inside the small cage were determined accurately by means of the DMC calculations. For $(p\text{-}H_2)_n$ and $(o\text{-}D_2)_n$ with $n = 1$ and 2, the ground-state energies are negative, implying that these states are truly bound and stable relative to the hydrogen molecule(s) at a large distance outside the cage (the zero of energy). These results suggest that double occupancy of H_2/D_2 in the cage is possible. The ground states of $(p\text{-}H_2)_3$ and $(o\text{-}D_2)_3$ in the small cage have large positive energies and are thus quasi-bound, metastable states. The spatial distribution of one and two hydrogen molecules inside the dodecahedral cavity was characterized with the help of several PDFs. They show that for $n = 2$ there is virtually a zero probability of finding a hydrogen molecule within ∼1.5 bohr from the center of the cage and the two hydrogen molecules occupy a shell whose width is less than 2 bohr. They are compressed at a mean distance of ∼4.85 bohr, and the interaction between them is repulsive. The 3D PDF of the centers of mass of the *p*-H_2 molecules for $n = 2$ has two distinct lobes centered at the minimum-energy configuration of two H_2 molecules in the small cage. This wave function localization is due to the corrugated H_2−cage interaction potential felt by the two H_2 molecules pressed close to the walls of the cage.

Investigations are in progress in our group of the quantum dynamics of several hydrogen molecules confined inside the large cage of the sII clathrate hydrate, and the results will be reported in the near future.

Acknowledgment. Z.B. is grateful to the National Science Foundation for partial support of this research through Grant CHE-0315508. The computational resources used in this work were funded in part by the NSF MRI Grant CHE-0420870.

References and Notes

(1) Sloan, E. D. *Clathrate hydrates of natural gases*; Marcel Dekker: New York, 1998.
(2) Mao, W. L.; Mao, H. K.; Goncharov, A. F.; Struzhkin, V. V.; Guo, Q.; Hu, J.; Shu, J.; Hemley, R. J.; Somayazulu, M.; Zhao, Y. *Science* **2002**, *297*, 2247.
(3) Mao, W. L.; Mao, H. K. *Proc. Natl. Acad. Sci. U.S.A.* **2004**, *101*, 708.
(4) Fichtner, M. *Adv. Eng. Mater.* **2005**, *7*, 443.
(5) Hu, Y. H.; Ruckenstein, E. *Angew. Chem., Int. Ed.* **2006**, *45*, 2011.
(6) Lokshin, K. A.; Zhao, Y.; He, D.; Mao, W. L.; Mao, H. K.; Hemley, R. J.; Lobanov, M. V.; Greenblatt, M. *Phys. Rev. Lett.* **2004**, *93*, 125503.
(7) Florusse, L. J.; Peters, C. J.; Schoonman, J.; Hester, K. C.; Koh, C. A.; Dec, S. F.; Marsh, K. N.; Sloan, E. D. *Science* **2004**, *306*, 469.
(8) Lee, H.; Lee, J.-W.; Kim, D. Y.; Park, J.; Seo, Y.-T.; Zeng, H.; Moudrakovski, I. L.; Ratcliffe, C. J.; Ripmeester, J. A. *Nature* **2005**, *434*, 743.
(9) Kim, D. Y.; Lee, H. *J. Am. Chem. Soc.* **2005**, *127*, 9996.
(10) Hester, K. C.; Strobel, T. A.; Sloan, E. D.; Koh, C. A.; Huq, A.; Schultz, A. J. *J. Phys. Chem. B* **2006**, *110*, 14024.
(11) Strobel, T. A.; Taylor, C. J.; Hester, K. C.; Dec, S. F.; Koh, C. A.; Miller, K. T.; Sloan, E. D., Jr. *J. Phys. Chem. B* **2006**, *110*, 17121.
(12) Patchkovskii, S.; Tse, J. S. *Proc. Natl. Acad. Sci. U.S.A.* **2003**, *100*, 14645.
(13) Sluiter, M. H. F.; Belosludov, R. V.; Jain, A.; Belosludov, V. R.; Adachi, H.; Kawazoe, Y.; Higuchi, K.; Otani, T. *Lect. Notes Comput. Sci.* **2003**, *2858*, 330.
(14) Alavi, S.; Ripmeester, J. A.; Klug, D. D. *J. Chem. Phys.* **2005,** *123*, 024507.
(15) Inerbaev, T. M.; Belosludov, V. R.; Belosludov, R. V.; Sluiter, M.; Kawazoe, Y. *Comput. Mater. Sci.* **2006**, *36*, 229.
(16) Lee, J. W.; Yedlapalli, P.; Lee, S. *J. Phys. Chem. B* **2006**, *110*, 2332.
(17) Alavi, S.; Ripmeester, J. A.; Klug, D. D. *J. Chem. Phys.* **2006,** *124*, 014704.
(18) Buch, V.; Devlin, J. P. *J. Chem. Phys.* **1993**, *98*, 4195.
(19) Lu, T.; Goldfield, E. M.; Gray, S. K. *J. Phys. Chem. B* **2003**, *107*, 12989.
(20) Lu, T.; Goldfield E. M.; Gray, S. K. *J. Phys. Chem. B* **2006,** *110*, 1742.
(21) Yildirim, T.; Harris, A. B. *Phys. Rev. B* **2003**, *67*, 245413.
(22) Xu, M.; Elmatad, Y.; Sebastianelli, F.; Moskowitz, J. W.; Bačić, Z. *J. Phys. Chem. B* **2006,** *110*, 24806.
(23) Hodges, M. P.; Wheatley, R. J.; Schenter, G. K.; Harvey, A. H. *J. Chem. Phys.* **2004**, *120*, 710.
(24) Mak, T. C. W.; McMullan, R. K. *J. Chem. Phys.* **1965**, *42*, 2732.
(25) McDonald, S.; Ojamäe, L.; Singer, S. J. *J. Phys. Chem. A* **1998**, *102*, 2824.
(26) Diep, P.; Johnson, J. K. *J. Chem. Phys.* **2000**, *112*, 4465.
(27) Jiang, H.; Bačić, Z. *J. Chem. Phys.* **2005**, *122*, 244306.
(28) Sebastianelli, F.; Elmatad, Y.; Jiang, H.; Bačić, Z. *J. Chem. Phys.* **2006**, *125*, 164313.

(29) Liu, S.; Bačić, Z.; Moskowitz, J. W.; Schmidt, K. E. *J. Chem. Phys.* **1994**, *101*, 10181.
(30) Liu, S.; Bačić, Z.; Moskowitz, J. W.; Schmidt, K. E. *J. Chem. Phys.* **1995**, *103*, 1829.
(31) Bačić, Z. *J. Chem. Soc., Faraday Trans.* **1997**, *93*, 1459.
(32) Hutson, J. M.; Liu, S.; Moskowitz, J. W.; Bačić, Z. *J. Chem. Phys.* **1999**, *111*, 8378.
(33) Bačić, Z.; Light, J. C. *Annu. Rev. Phys. Chem.* **1989**, *40*, 469.
(34) Mandziuk, M.; Bačić, Z. *J. Chem. Phys.* **1993**, *98*, 7165.
(35) Bačić, Z.; Light, J. C. *J. Chem. Phys.* **1986**, *85*, 4594.
(36) Bačić, Z.; Light, J. C. *J. Chem. Phys.* **1987**, *86*, 3065.
(37) Jankowski, P.; Szalewicz, K. *J. Chem. Phys.* **1998**, *108*, 3554.
(38) Jankowski, P.; Szalewicz, K. *J. Chem. Phys.* **2005**, 123.
(39) Anderson, J. B. *J. Chem. Phys.* **1975**, *63*, 1499.
(40) Anderson, J. B. *J. Chem. Phys.* **1976**, *65*, 4121.
(41) Hammond, B. L.; Lester, W. A., Jr.; Reynolds, P. J. *Monte Carlo Methods in Ab Initio Quantum Chemistry;* World Scientific: Singapore, 1994.
(42) Suhm, M. A.; Watts, R. O. *Phys. Rep.* **1991**, *204*, 293.
(43) Gregory, J. K.; Clary, D. C. Diffusion Monte Carlo studies of water clusters. In *Advances in Molecular Vibrations and Collision Dynamics;* Bowman, J. M., Bačić, E., Eds.; JAI Press, Inc.: Stamford, CT, 1998; Vol. 3, p 311.
(44) Whaley, K. B. Spectroscopy and microscopic theory of doped helium clusters. In *Advances in Molecular Vibrations and Collision Dynamics;* Bowman, J. M., Bačić, E., Eds.; JAI Press, Inc.: Stamford, CT, 1998; Vol. 3, p 397.
(45) Sarsa, A.; Schmidt, K. E.; Moskowitz, J. W. *J. Chem. Phys.* **2000**, *113*, 44.